A New System for Measuring the Auto-Fluo Changes in Age-Related Macula Degeneration after Intravenous Injection of Bavecizumab Medicine

Mohammad Faraji, Mohammad Norouzi Fard, Saeed Mirghasemi

Abstract*: *In aged people, age-related macula degeneration is the second prevalent disease after diabetes which causes blindness. The only cure for age-related macula degeneration is the Bavecizumab intravenous medicine injection. To prove this treatment, the number of dead cells in macula area should be considered. In this paper, to obtain the number of dead cells, a novel system has been presented for measuring the existing auto fluorescence in macula area of retinal images. This combinational system is composed from three parts; pre-processing of retinal, processing the images, and understanding the images. The pre-processing level, includes eliminating margins, and reversing retina image. In processing level, the image is segmented, and features are extracted, where the segmentation has been done using techniques like morphology, dynamic thresholding and connected components. The specifications of target areas are the Euclidian distance to the center of the image, and density. In the understanding level of image, collecting the specifications of each class, macula area and the measurable parameter for evaluating the amount of auto fluorescence is obtained which is useful for determining the number of dead cells in macula area. The results are concluded using probabilistic analysis including linear regression and correlation between data. The method is tested on a database composed of 34 retina images belonging to patients of age-related macula degeneration.

Index Terms*: *Age-related macula degeneration, Connected components, Morphology, Macula, , Retina image.

I. INTRODUCTION

Retina is a sensitive narrow membrane which is located in the backside of eyeball. Light beams that hit retina become neural messages which are transferred to the brain through optic nerves, and are interpreted. In retina, there are various types of photoreceptor cells which have different sensitivity to light. Their arrangement in retina is so that their number is more in the central area of retina (Macula). Therefore, when a person looks right to an object, the image of that object reflects directly on the macula, where the number of photoreceptor cells are more, and thereby the object would be observed more clearly. In Fig. 1 different components of an eye and the location of retina is shown. In order to study the effects of AMD[1] on retina we should survey different types of it. AMD is divided to types: dry AMD, and wet AMD. The dry type is the case for approximately 90% of patients (Fig. 2). In this level, yellow sediments are formed in the central area of vision. Fortunately, dry AMD has a slow progress and may cause poor or severe dimness in vision. In the beginning of this level, especially when the illness is in one eye, one may not notice the disorder in vision, and could do the daily tasks normally. Some suggest using vitamins and antioxidants to prevent the illness progress in this level.

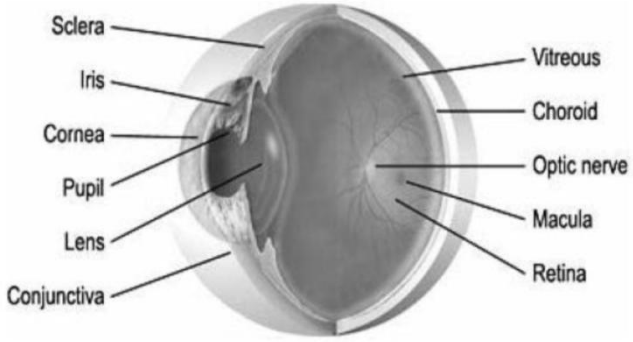

Fig. 1: An incision of eye and its components

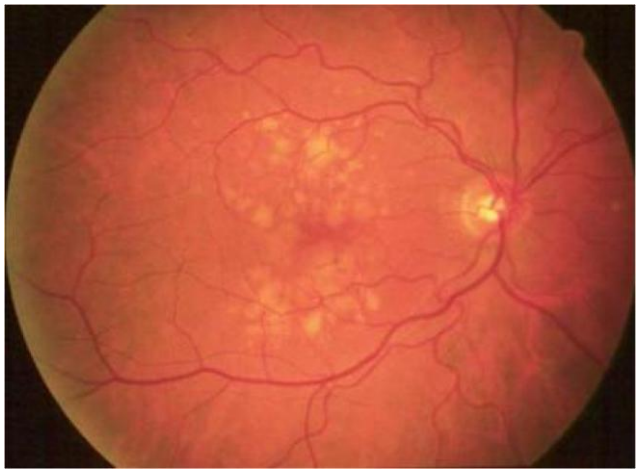

Fig. 2: The retina image of a patient suffering from the dry AMD.

The wet AMD kind which is observable in Fig. 3, is common in 10% of patients, but 90% of severe vision disorders are in this category. In this stage, improper blood vessels grow beneath the retina area of macula. Since these vessels are too fragile, they cause blood and liquid leaking to the underneath area of macula, and finally loss of sensitive cells in this area which is the reason for severe loss of vision. One of the primary signs of wet AMD is seeing straight lines crooked or wavelike which is the result of liquid leakage and edema in the central area of macula. Also, patient sometimes lose the central vision critically which is the result of

Revised Manuscript Received on December, 2012.

Mohammad Faraji, Department of Computer & IT Engineering, Islamic Azad University, Parand Branch, Tehran, Iran.
Mohammad Norouzi Fard, Department of Computer Engineering, Islamic Azad University, Science & Research Branch, Tehran, Iran.
Saeed Mirghasemi (Corresponding Author), Department of Computer & IT Engineering, Islamic Azad University, Parand Branch, Tehran, Ira

bleeding in the vision central area.

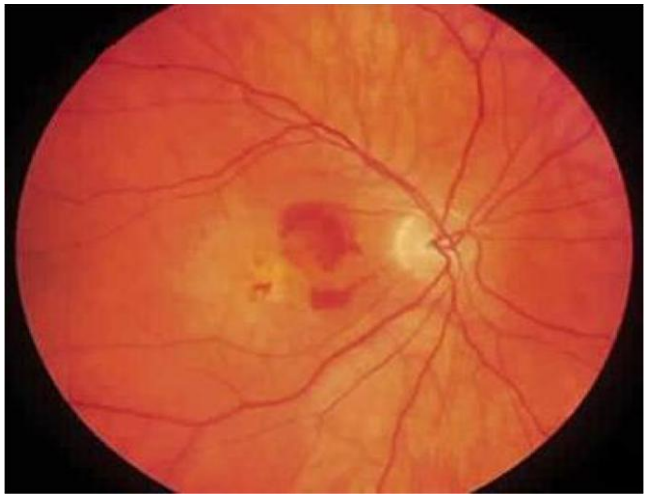

Fig. 3: The retina image of a patient suffering from the wet AMD.

Extensive researches have been done on the wet AMD which indicate that image analysis would considerably improve the diagnostic value of retina images. In fact, emersion of eye imaging equipment for AMD diagnosis has decreased the costs and increased accuracy in illness diagnosis.

Now a new modern commodious system of retina images could be proposed to facilitate diagnosis for physicians. Such a system should be capable of detecting primary signs of retina disease, and provide an objective diagnosis based on defined criteria with oculists. It is expectable that the proposed system would not only increase capability and efficiency of oculist during examination, but also could be an automatic tool for supervising a wide range of AMD patients.

Intraretinal hypo cells are an observable sign for AMD disease, and also a sign for existence of coexistent retinal edema in macula area. If these cells attend at yellow part of retina (macula), dead cell, edema and exudates are the main reasons of non-proliferative blindness. Dead cells, edema and retinal exudates are in the central region of clinical signs which are closely related to blindness. Exudates are pictured with vessel destruction splotches, and usually are shown like splotches with random yellow distances which are of different sizes and shapes. In fact, the size and distribution of splotches are variant during the disease progress. In this research work we have focused on recognition of splotches, dead cells and edema in macula area as primary signs. For there is the possibility of companionship of collective splotches and retina edema. Unlike edema, exudates are more observable in color images of retina. In many captured images which should be repeated annually, seeing exudates in retina is both expensive and possible to be along with human mistake. The main goal in this research is to propose a new method to classify dead cells in optic disks of auto fluorescence images, and analyse the number of them according to statistics methods. In this regard, we should obtain the whole area related to optic disk.

The previous researches on the retina could be divided two general categories; first, experiments and researches on angiography color images of retina, and second, gray images resulted from auto fluorescence effects. The later is mostly used for edema/dead cells recognition. In literature automatic detection of optic disk in AMD has not been extensively considered. In this paper, localization of optic disk has been thought over. Similar research works has been done in [1] and [2]. Generally, previous researches are divided to two groups; the first one tries to detect the blind spot utilizing different methods, and the second one, tries to detect vessels. For instance, one step of edge detection, and one step of circular Hough transform was done to localize the blind spot. The algorithm is starting with localizing the selected region for the blind spot. This was implemented as a region of 180×180 pixels when the highest 2% gray level of red color was defined as retina. Next, the Sobel operator has been applied for detection of edge spots in the selected region. Therefore, edge lines was detected using circular Hough transform i.e. the gradient of image was calculated, and the best circular circle was nominated. This kind of approaches are totally time consuming, and are dependent to shape condition of the blind spot which is obtainable all the time. In addition, to provide an acceptable solution, most of edge detector algorithms because of fuzzy edges, incompatible image contrast, and vagueness in edge features are failed. In [3] the blind spot has been localized using mathematical morphology filtering and watershed transformation techniques. Initially, local gray level variance intensity of adjacent pixels has been calculated to estimate the locus of the blind spot. This approach is only effective in normal images in which the retina image doesn't have fat exudates. Therefore, a shade correction operator has been employed to eliminate the slow background differences, and reduce the contrast of injuries resulted from fat discharges. In this correspondence, first they have estimated slow background differences with sequential filters, and then the difference between the values of the original image and background estimation has been calculated.

After pre-processing steps, the watershed transformation has been applied to localize the possible location of the blind spot. Since the blind spot represents a bright region, and blood vessels appears darkly in the gray level image of retina, gray level changes inside the blind spot region is very high. This changes has been firstly implemented using a closing morphological operation to ease the afterwards watershed operation. Some of the proposed methods in the mentioned papers have been utilized to present a novel method for macula detection (optic disk).

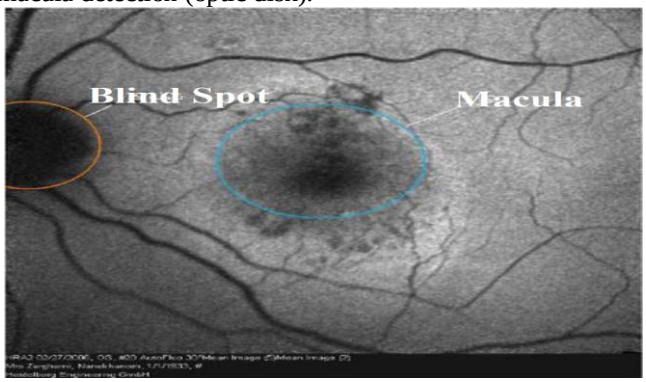

Fig. 4: Auto fluorescence image of retina in which (optic disk) and blind spot are depicted.

II. THE UTILIZED METHODS IN TRIPLE STEPS OF MACHINE VISION

First, a brief explanation has been brought regarding low level image processing.

Next, we explain how to analyze retina images which were obtained from the first step, and in the end the perception is formed based on the utilized analysis.

A. low-level image analysis

Since image data bases in this area are hard to achieve, we did our experiments on a data base containing 36 retina images of patients of AMD. In fact, they are 18 pairs of images, with each pair belonging to a patient, and an improper pair which we set aside for the next processing implementations. The utilized images have been obtained from the HRA2 auto-Fluo imaging device of Noor and Labbafi Nezhad ophthalmology clinic. A sample of retina image after loading is shown in Fig. 6. This image belongs to a patient of AMD which is under treatment via injection. The original retina images of patients contains a waste area in the bottom of the image. First, this waste area is eliminated, and all images are converted to 768*768 images [7] (Fig. 7). Next, considering that we want to detect background regions in the afterward levels, we subtract all pixels of the image from 255 [8]. Doing so, the images are getting ready for processing in image analysis step. The obtained image in Fig. 8 is the output of the pre-processing level and is ready for the next processes.

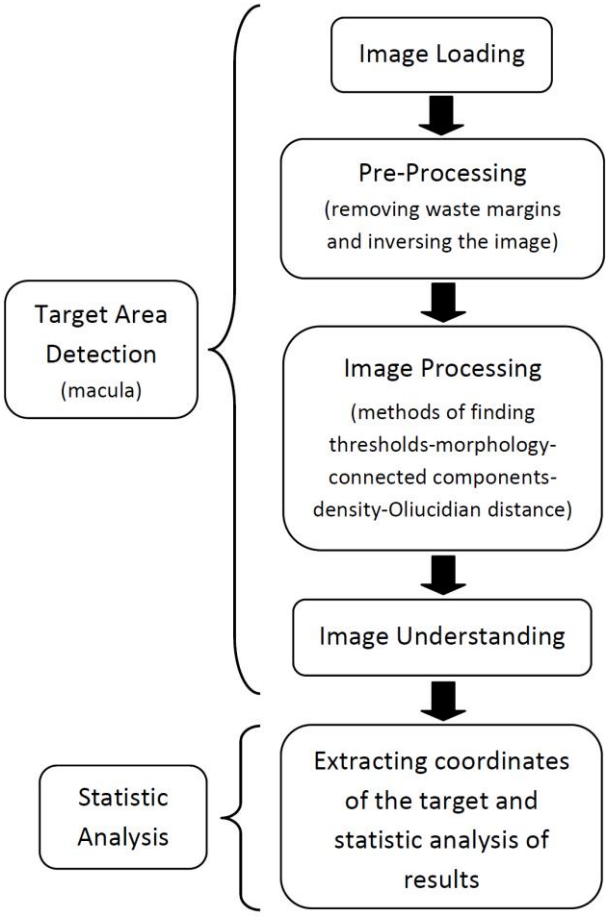

Fig. 5: The block diagram of the proposed method.

B. Image Analysis

After the primary processing the obtained image is getting segmented so we could obtain the mentioned areas for detecting the dead cells. According to our experiments on our image dataset we found that the Otsu's method [4] would lead us to best results [5]. After segmentation via Otsu's method the gray level image turns to a binary image (Fig. 9).

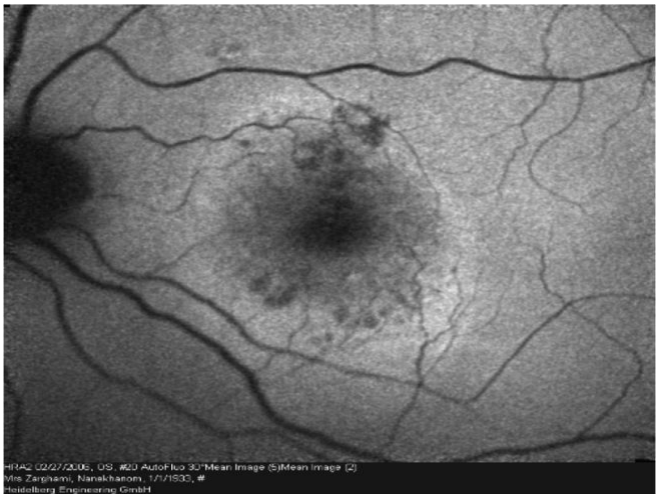

Fig. 6: The original retina image of Auto-Fluo type.

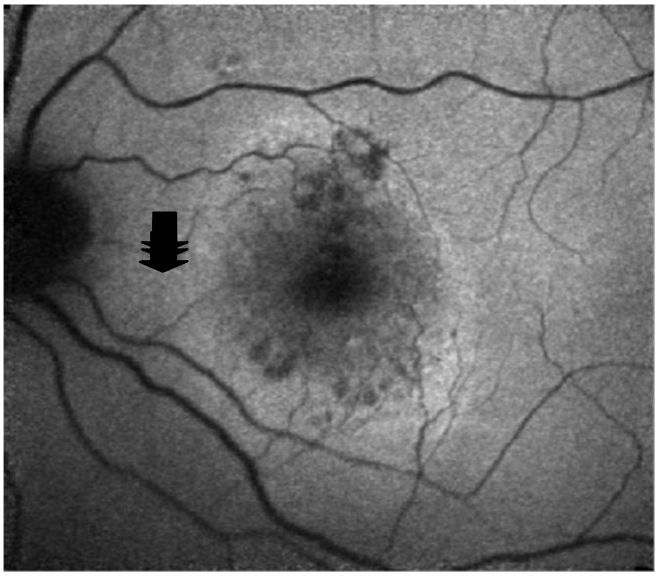

Fig. 7: The retina image after removing the waste margins.

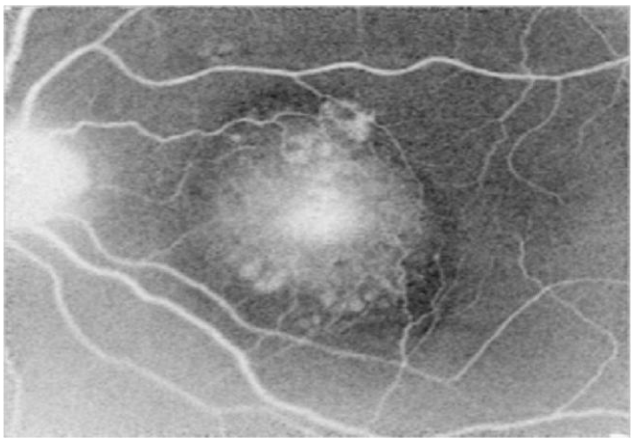

Fig. 8: The output of pre-processing level.

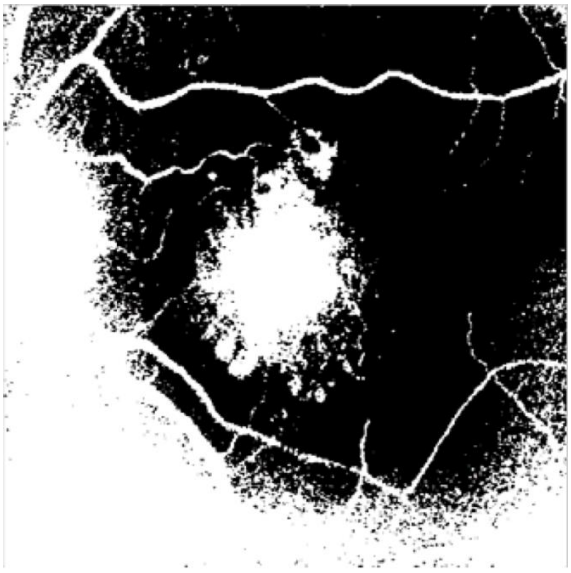

Fig. 9: An estimate of the concerned areas.

In this level, the concerned areas are obtained approximately, but the obtained areas have overlap, and are not separable. In the next level, to approximately separate the areas, and also to eliminate very small regions which are noise in fact, we have used morphological methods [6]. In morphology we have dilation and erosion. These two operator are the base for most of morphological tasks. Imagine that A and B with components of a=(a1,a2), b=(b1,b2) are sets in Z2. Transformation of A2 with x=(x1,x2) is shown with (A)x which is defined as follows:

$$(A)_x = \left\{c \middle| c = a + x \ , \ for \ \ a \in A\right\} \tag{1}$$

The symmetry of B which is shown with $\hat{B}$, is determined in terms of (2):

$$\hat{B} = \left\{x \middle| x = -b \ \ for \ \ b \in B\right\} \tag{2}$$

In (3) the complement of set A has been represented:

$$A^c = \left\{x \middle| x \neq A\right\} \tag{3}$$

Finally, the differentiation of sets A and B is shown with $A - B$ which is represented as (4):

$$A - B\left\{x \middle| x \in A \ , x \notin B\right\} = A \cap B^c \tag{4}$$

Assuming A and B are sets in Z^2, and Φ as an empty set, dilation of A and B is shown with $A \oplus B$, and is defined as:

$$A \oplus B = \left\{ x \middle| (\hat{B})_x \cap A \neq \phi \right\} \tag{5}$$

Therefore, the procedure of dilation includes obtaining the symmetry of B around its origin and then transforming this symmetry with x so that $\hat{B}_x$ could be obtained. Then, dilation of A with B is the set of all x in which ($\hat{B}_x$) and A have overlap at least in a non-zero element. According to this change, we could re-write (5) as follows:

$$A \oplus B = \left\{ x \middle| \left[(\hat{B})_x \cap A \right] \subseteq A \right\} \tag{6}$$

B usually is known as structure element in dilation and other applications of morphology.

(5), is not the only definition of dilation. However, this definition has an obvious superiority to other definitions, because whenever we look at the B structure element as a convolution mask, this definition is more intuitive. Although, dilation is based on sets operations and convolution is based on mathematics operations, but flipping of B around its origin and then its successive movement while it is being slid on all images of A, is in the same manner to convolution procedure. Therefore, first we do the erosion morphology, and as a result very small regions will be omitted (Fig. 10), and also connected areas would be separated. At the end, due to elimination of some parts after erosion, we do the dilation morphology to retrieve them (Fig. 11). Regarding our experiments on the image dataset and the obtained results, the dilation and erosion morphology have been done using a circular mask with radiation of 10 pixels. To extract features from the output image of erosion implementation, different regions must be distinguished. For this, we need to label connected components on the image.

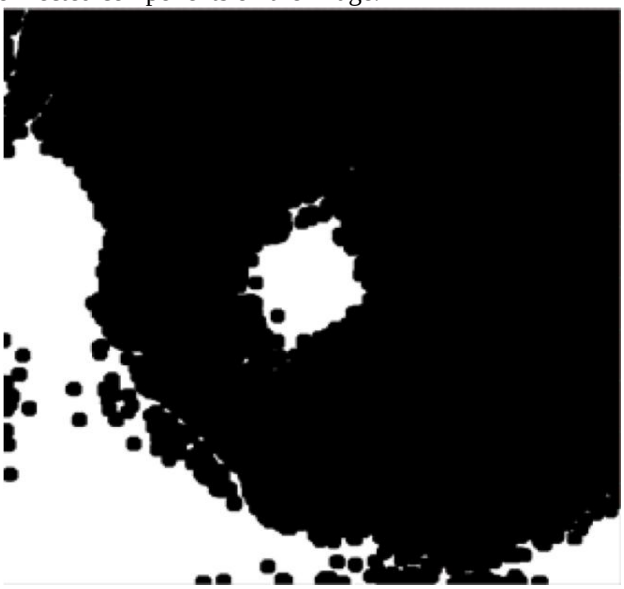

Fig. 10: Erosion morphology.

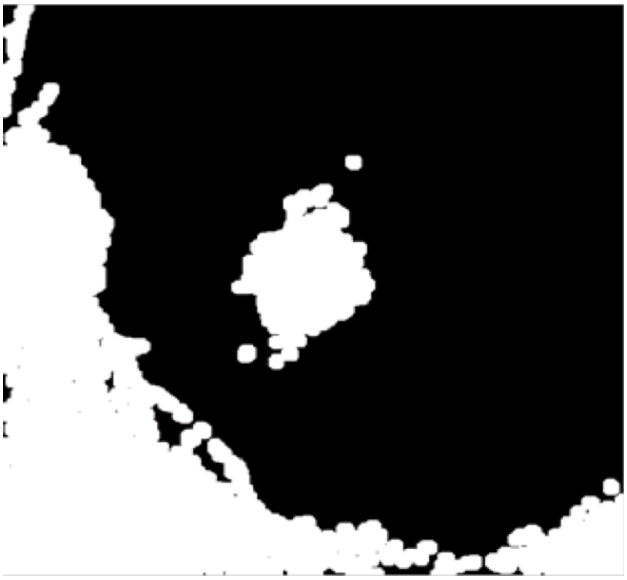

Fig. 11: Dilation morphology.

In this correspondence, we begin labelling pixels regarding 4-connectivity or 8-connectivity. Since in this special research using 8-connectivity would cause blending of previously separated regions, we use 4-connectivity to label pixels, and classify them. This will avoid the previously separated regions to be taken into account as a single region. Next, we paint them for better observation and classification. Then we calculate parameters like coordinates of the embedding rectangles of the segments, and the number of pixels in each segment in the obtained segments from the previous level. The outputs of this analysis are rectangular regions which are detected as candidates for macula region. The center of each segment is specified in Fig. 11.

For each detected region, we calculate two features; Euclidian distance of each class from the center of image, and its density. The density in a candidate region is the value of division of the number of dark color pixels in that region and the total number of pixels in it. Regarding the carried out clinical experiments in presence of ophthalmology specialist we found that the best relationship between these features for detecting macula is when the weight value of the Euclidian distance is two times the density one. At the end, for candidate segments we obtain a value as suitability. Macula region is the region with the highest suitability. The proposed area for macula in Fig. 12 is specified with a blue circle.

It should be noticed that the proposed steps has been presented for analyzing gray level images of retina of AMD disease, assuming that the optometrist mistake in imaging procedure is at the lowest level.

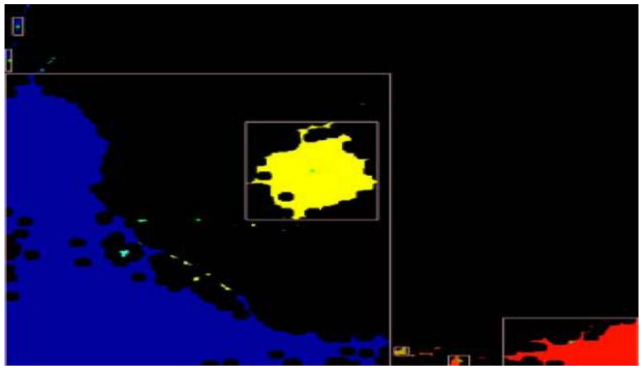

Fig. 12: Classification and specification of candidates regions.

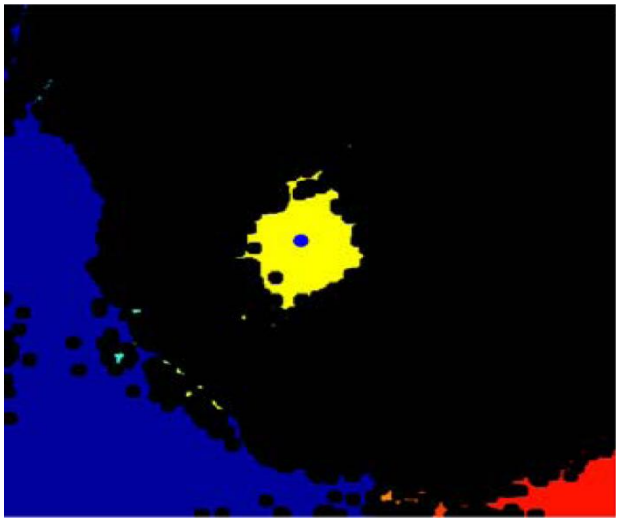

Fig. 13: Specification of macula region.

III. IMAGE UNDERSTANDING AND ANALYSIS OF RESULTS

We use the outputs of the analyzing step as the inputs of this step. Data from the previous level are actually the number of dead cells in the images of AMD before and after treatment with injection of Bavecizumab medicine. Therefore, the data related to results are categorized in two classes of before and after treatment. These data are gathered in Table 1.

The results in table 1 indicate that the amount of reduction in the damaged cells of macula region in images of our database is 15134 in average. Also, the variance of results is 2366854464 before treatment, and 4341813191 after that. It should be noticed that the value of standard deviation is 48650.32851 before treatment, and 65892.43652 after treatment. To implement different steps of the proposed method we have used MATLAB software.

Table I: Comparing the number of damaged cells before and after treatment.

Row	Number of cells before treatment	Number of cells after treatment
1	20508	959
2	153000	904
3	127000	24511
4	13460	13498
5	59502	107
6	72884	7638
7	385	944
8	26785	115
9	105000	276000
10	2824	391
11	203	312
12	2126	1103
13	231	21637
14	18219	11049
15	498	666
16	17898	2061
17	14936	16253

IV. RESULT ANALYSIS

One method for analyzing is regression. In linear regression the dependent variable, y_i, is a combination of coefficients (parameters). It is not necessary for it to be linear to independent variables. For example, the simple regression analysis (straight line) with N points, the independent variable, x_i, and β_0 and β_1 in (7) is linear:

$$y_i = \beta_0 + \beta_1 x_i + \in_i, i = 1,..., N \quad (7)$$

In multiple regression (sagittal), there is more than one independent variable which has been indicated in (8):

$$y_i = \beta_0 + \beta_1 x_i + \beta_2 x_i^2 + \in_i, i = 1,..., N \quad (8)$$

Although (8) is not linear to dependent variable, x_i, it is still a linear regression, because y_i is a linear combination of β_0 and β_1. In both cases $\in_i$ is error value, and the index i indicates the number of each observation (each pair of x_i and y_i). Having a set of these numbers, (9) could be obtained:

$$y_i = \hat{\beta}_0 + \hat{\beta}_1 x_i + e_i, i = 1,..., N \quad (9)$$

The term e_i is called remained: $e_i = y_i - \hat{y}_i$. The common method for calculating parameters is the least square. In this method parameters are obtained with minimizing the following equation:

$$SSE = \sum_{i=1}^{N} e_i^2 \quad (10)$$

Regarding the simple regression, the achieved parameters are equal to the following equations:

$$\hat{B}_1 = \frac{\sum(x_i - \bar{x})(y_i - \bar{y})}{\sum(x_i - \bar{x})^2} \quad (11)$$

$$\hat{B}_0 = \bar{y} - \hat{b}_1 \bar{x} \quad (12)$$

in which $\bar{x}$ and $\bar{y}$ are the averages of x and y [9]. The meaning of solidarity is existing a logical relationship between data [10].

V. CONCLUSIONS

Since a few work have been done in this field, there is not an standard image database. Therefore, we were not able to make a proper comparison in our results. In this paper a new method was presented to detect the optic disk in AMD patients before and after treatment. Among these 36 images, we were able to examine 34 images for macula detection, and the macula has been detected in 92.4% of images correctly. At the end, regarding the analysis method, clinical investigations, and the carried out implementations, it has been unfolded that this therapy method is efficient in edema reduction of macula but we could not find a logical relevance for vision enhancement in patients.

REFERENCES

1. Z. Liu, C. Opas, S. Krishnan, "Automatic image analysis of fundus photograph", In proceedings of 19th IEEE Int. Conf. on Eng. in Medicine and Biology Society, pp.524-525, 1997.
2. B. Ege, O. Larsen, O. Hejlesen, "Detection of abnormalities in retinal images using digital image analysis", In proc. of the 11th Scandinavian Conf. on Ima. Proc., pp.833-840, 1999.
3. T. Walter, J. Klein, P. Massin, A. Erginary, "A contribution of image processing to the diagnosis of diabetic retinopathy, detection of exudates in colour fundus images of the human retina", IEEE Trans. on Media Imaging., 21(10):1236-1243, 1998.
4. N. Otsu, "A threshold selection method from gray-level histograms", IEEE Trans. on Systems, Man, and Cybernetics., Vol.9, No.1, pp.62-66, 1979.
5. R. M. Rangayyan, "Biomedical image analysis", University of Calgary, Alberta, Canada,'book', 2005.
6. R. C. Gonzalez, R. E. Woods, "Digital image processing", 2nd.Ed., Prentice Hall Upper Saddle River, New Jersey, 2001.
7. Li. Huiqi, Opas Chutatape, "Automated feature extraction in color retinal images by a model based approach", IEEE Trans. on Bio. Engi., Vol.51, No.2, Feb. 2004.
8. N. Katz, M. Goldbaum, et al., "An image processing system for automatic retina diagnosis", SPIE, Vol.902, 1988.
9. J. Hope Mccoll, "Multivariate probability", Paperback – Jan. 2002.
10. Z. Peebles Peyton, "Probability, random variables and random signal principles", 2009.

AUTHORS PROFILE

Mohammad Faraji has received his B.Sc. degree in computer engineering from Tarbiat Moalem University in 1999, and his master's degree in computer science from Tehran University in 2002. His research interests are algorithm design, data base programming, data mining, and medical image processing. He has been a faculty member at the department of computer and IT engineering since 2006.

Mohammad Norouzi Fard has received his M.Sc. degree from Islamic Azad University, Science and Research branch, in Artificial Intelligence. He is now a lecturer at Jame University of Applied Science and Technology.

Saeed Mirghasemi has received his B.Sc. and M.Sc. Degree in Electrical Engineering from Semnan University and MUT in Iran in 2006 and 2009 respectively. He is currently with Islamic Azad University Parand branch as a lecturer. He has won several research grants, and has several published journal and conference papers in the field of intelligent image and signal processing. His research interests include pattern recognition, image processing and machine learning with emphasis on Kernel Methods, Evolutionary Computation and Optimization Techniques.